Table IV. Mulliken Population Analysis

metal AO	sym Mo	sym Cr	unsym Mo	unsym Cr
s	0.16	0.25	0.16	0.25
p_x	0.11	0.18	0.12	0.19
p_y	0.11	0.18	0.12	0.19
p_z	0.25	0.38	0.22	0.36
d_{z^2}	0.85	0.73	0.84	0.73
$d_{x^2-y^2}$	0.52	1.05	0.51	1.05
d_{xy}	0.73	0.47	0.73	0.46
d_{xz}	0.84	0.81	0.84	0.80
d_{yz}	0.84	0.81	0.84	0.80

ticipate in the same occupied MO's. A Mulliken population analysis (Table IV) reveals that the p_z orbital has a significantly higher population than the corresponding p_x and p_y orbitals. The calculations indicate that these changes in energy are of sufficient magnitude to cause substantial interaction.

Fock Matrix Elements. Comparing the Fock matrix elements between the equatorial and axial oxygen AO's and the metal AO's, we observe a large dissimilarity only for the oxygen 2s orbitals and the metal p_z orbitals. For chromium tetraperoxide $F_{uv}(\mathrm{eq}) = -0.015$ and $F_{uv}(\mathrm{ax}) = -0.412$ for the metal p_z and oxygen 2s orbitals. For molybdenum tetraperoxide similar differences are observed. this, once again, indicates a significant difference in the strength of the interaction between the axial and oxygen 2s AO's and the metal p_z orbital. The greater interactions (S_{uv}, P_{uv}, and F_{uv}) will lead to geometric distortions in the direction observed experimentally. No other orbital interactions satisfy the criterion of large differences for these three properties.

Atomic Bond Index. A comparison of the atomic bond indices between the symmetric and asymmetric structures is informative in that it is a summation of the various orbital interactions (and thus different from the previous three criterion) for the two atoms. Perturbation of the chromium tetraperoxide from the symmetric to asymmetric configuration leads to a small change in the chromium–equatorial oxygen bond index, from 0.66 to 0.65. However, the analogous chromium–axial oxygen bond index changes more substantially from 0.65 in the symmetric form to 0.69 in the asymmetric. For $Mo(O_2)_4^{2-}$ the changes are inconclusive since the differences are smaller and cancel each other out. Thus, at least for chromium the calculations indicate that the potential energy surface is softer for chromium–equatorial oxygen bond distortion than chromium–axial oxygen bond distortion. Thus, the chromium–axial oxygen bond can be distorted in a way that will increase its strength, with relative disregard for the chromium–equatorial oxygen bond, which is insensitive to this distortion mode. The weaker interactions of the equatorial oxygen atoms with the central metal atom, which we have pointed out throughout this paper, would seem to dictate just such a soft potential energy surface for this distortion.

Jahn–Teller Mechanism. We discounted a first-order Jahn–Teller distortion since no partially filled degenerate MO's exist in chromium tetraperoxide and the molybdenum analogue is a closed-shell molecule. A second-order Jahn–Teller distortion was deemed to be inoperative due to the presence of a good HOMO–LUMO gap, and the gap was rather insensitive to the geometrical distortion.

Finally, we note that the INDO calculations are approximate. Nevertheless they do produce a distortion of the bonding as observed in experiments. Furthermore, they provide a reasonable explanation for this distortion.

Conclusions

The difference between metal–oxygen bond lengths in molybdenum and chromium tetraperoxide is due in large part to the difference in the strength of interaction between the 2s AO's of axial and equatorial oxygen atoms with the metal p_z AO. Poorer overlap for the equatorial 2s orbitals combined with a much larger bond order for the axial 2s orbitals leads to a stronger interaction and provides the driving force for the ensuing distortion to dissymmetric coordination. A good energy match between the metal p_z and oxygen 2s orbitals is obtained due to the high oxidation state of the metal lowering its AO's while the negative charge on the peroxide raises the energy of its orbitals. A large bond order, significant population of the metal p_z orbital, and the Fock matrix elements all point to a reasonable energy match involving the metal p_z orbital. Additionally, a comparison of the change in atomic bond index as the distortion occurs indicates that the Cr–Oe bond is insensitive while the Cr–Oa bond strengthens more significantly.

Acknowledgment. Helpful discussions with A. Cameron and D. Swieter of the University of Florida are gratefully acknowledged. This work was supported in part through U.S. Army Research Center Grant No. DAAA15-85-C-0034.

Contribution from the Department of Chemistry,
Auburn University, Auburn, Alabama 36849

Theoretical Study of the Interaction of NH_3 with the Boron Hydrides BH_3, B_3H_7, B_4H_8, and B_5H_9 and the Carboranes $C_2B_3H_5$ and $C_2B_3H_7$

Michael L. McKee

Received June 27, 1988

Geometries and energies of Lewis base adducts of ammonia with several boron hydrides and carboranes have been calculated by ab initio methods. Geometries were optimized at the HF/3-21G level, and single-point calculations were made at the MP2/6-31G* level. The B–N bond strength is largest when NH_3 is coordinated to a BH_2 unit that forms a three-center two-electron bond to the remainder of the molecule. A weaker B–N bond results when the BH_2 unit forms another two-center two-electron bond, while the weakest B–N bond occurs when the NH_3 is coordinated to a boron center that is already coordinatively rich.

Nucleophiles are known to form adducts with boron hydrides[1-3] and to a lesser extent with carboranes.[4,5] For the reactive boron hydrides B_3H_7 and B_4H_8, the structures of the free boron hydrides are often assumed to be the same as those of their adducts, since the former have not been isolated. However, the geometries of many adducts are radically different from the unadducted form

---

[1] Greenwood, N. N. In *Comprehensive Inorganic Chemistry*; Trotman-Dickenson, A. F., Ed.; Pergamon: New York, 1973; Vol. 3.

[2] Shore, S. G. *Pure Appl. Chem.* **1977**, *49*, 717–732 and reference cited therein.

[3] Fehlner, T. P.; Housecroft, C. E. In *Molecular Structures and Energetics*; Liebman, J. F., Greenberg, A., Eds.; Verlag Chemie International: Deerfield Beach, FL, 1984; Vol. 1.

[4] Onak, T. In *Comprehensive Organometallic Chemistry*; Wilkinson, G., Stone, F. G. A., Abel, E., Eds.; Pergamon: Oxford, England, 1982; Vol. 1, pp 411–457.

[5] Lew, L.; Haran, G.; Dobbie, R.; Black, M.; Onak, T. *J. Organomet. Chem.* **1976**, *111*, 123–130.

0020-1669/88/1327-4241$01.50/0 © 1988 American Chemical Society

Table I. Absolute Energies (hartrees) of Borane– and Carborane–NH_3 Adducts[a]

		3-21G	6-31G*	MP2/6-31G*[b]
	BH_3	−26.237 30	−26.390 01	−26.464 22
	NH_3	−55.872 20	−56.182 50	−56.351 92
	B_2H_6	−52.497 81	−52.812 37	−52.992 41
	$BH_3{\cdot}NH_3$	−82.166 31	−82.611 20	−82.872 27
1a	$B_3H_7{\cdot}NH_3$	−133.530 87	−134.278 45	−134.727 29
1b	$B_3H_7 + NH_3$	−133.465 69	−134.232 21	−134.659 00
1c	$B_3H_7{\cdot}NH_3$	−133.518 14	−134.266 60	−134.704 18
1d	$B_3H_7 + NH_3$	−133.466 33	−134.232 75	−134.650 87
1e	$B_3H_7 + NH_3$[c]	−133.457 21	−134.229 82	−134.665 44
2a	$B_4H_8{\cdot}NH_3$	−158.632 56	−159.525 95	−160.070 20
2b	$B_4H_8 + NH_3$	−158.567 37	−159.479 97	−160.001 36
2c	$B_4H_8{\cdot}NH_3$	−158.628 70	−159.518 06	−160.039 39
2d	$B_4H_8 + NH_3$	−158.575 09	−159.481 69	−159.981 53
2e	$B_4H_8 + NH_3$[d]	−158.540 31	−159.462 22	−160.001 22
3a	$B_5H_9{\cdot}NH_3$[e]		−184.753 56	−185.382 11
3b	$B_5H_9 + NH_3$	−183.661 41	−184.719 34	−185.325 09
3c	$B_5H_9 + NH_3$[f]	−183.694 16	−184.760 57	−185.400 50
4a	$C_2B_3H_5{\cdot}NH_3$	−207.690 46	−208.836 56	−209.490 32
4b	$C_2B_3H_5 + NH_3$	−207.639 24	−208.803 10	−209.438 64
4c	$C_2B_3H_5 + NH_3$	−207.691 23	−208.866 28	−209.528 73
5a	$C_2B_3H_7{\cdot}NH_3$	−208.787 68	−209.955 75	−210.652 32
5b	$C_2B_3H_7 + NH_3$	−208.778 29	−209.965 86	−210.643 17
5c	$C_2B_3H_7{\cdot}NH_3$	−208.725 86	−209.898 31	−210.610 71
5d	$C_2B_3H_7 + NH_3$	−208.780 09	−209.974 75	−210.667 70

[a] Geometries and energies for NH_3, BH_3, and B_2H_6 at the 3-21G level have been reported previously: Whiteside, R. A.; Frisch, M. J.; Pople, J. A. *Carnegie-Mellon Quantum Chemistry Archive*, 3rd ed.; Carnegie-Mellon University: Pittsburgh, PA, 1983. [b] Frozen core approximation has been used. [c] Doubly bridged species. [d] Quadruply bridged species. [e] The geometry was taken from the C_2 symmetry structure $B_5H_{10}^-$, where a NH_3 group replaces a hydride. The B–N bond was assumed to be 1.68 Å. [f] Optimum B_5H_9 structure in C_{4v} symmetry.

as indicated for the free and adducted forms of the boron hydrides[2] B_5H_9 and B_6H_{10}:

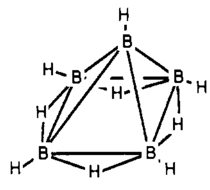

B_5H_9

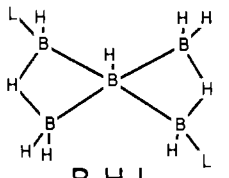

$B_5H_9L_2$

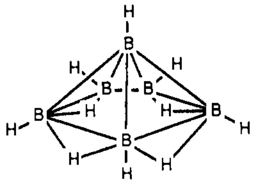

B_6H_{10}

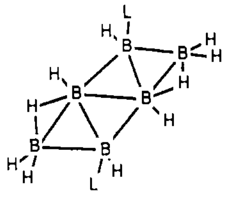

$B_6H_{10}L_2$

In general the more compact nido and closo structures are converted to more open hypho structures, which are characterized by one or more vacant orbitals on boron capable of accepting a pair of electrons from a nucleophile. Since classical forms of electron-deficient molecules have a greater percentage of two-center two-electron bonds with corresponding vacancies on boron, the nucleophile can stabilize this form, in a sense trapping the electron-deficient molecule in a classical structure.

The structure of the classical form is of interest since rearrangements of boron hydrides and carboranes have been suggested to go through classical transition states.[6] One such reaction is the skeletal rearrangement in B_5H_9, which takes place at elevated temperature in the gas phase.[7] Interestingly, the reaction occurs rapidly at room temperature in a coordinating solvent, where presumably the solvent lowers the barrier height by stabilizing the transition state.

Table II. Relative Energies (kcal/mol) with Respect to Various Reference Compounds

		3-21G	6-31G*	MP2/6-31G*
	$2BH_3$	0.0	0.0	0.0
	B_2H_6	−14.6	−20.3	−40.2
	$BH_3 + NH_3$	0.0	0.0	0.0
	$BH_3{\cdot}NH_3$	−35.6	−24.3	−35.2
1a	$B_3H_7{\cdot}NH_3$	0.0	0.0	0.0
1b	$B_3H_7 + NH_3$	40.9	29.0	42.9
1c	$B_3H_7{\cdot}NH_3$	8.0	7.4	14.5
1d	$B_3H_7 + NH_3$	40.5	28.7	48.0
1e	$B_3H_7 + NH_3$	46.2	30.5	38.8
2a	$B_4H_8{\cdot}NH_3$	0.0	0.0	0.0
2b	$B_4H_8 + NH_3$	40.9	28.9	43.2
2c	$B_4H_8{\cdot}NH_3$	2.4	5.0	19.2
2d	$B_4H_8 + NH_3$	36.1	27.8	55.6
2e	$B_4H_8 + NH_3$	57.9	40.0	43.3
3a	$B_5H_9{\cdot}NH_3$		0.0	0.0
3b	$B_5H_9 + NH_3$		21.5	35.8
3c	$B_5H_9 + NH_3$		−4.5	−11.5
4a	$C_2B_3H_5{\cdot}NH_3$	0.0	0.0	0.0
4b	$C_2B_3H_5 + NH_3$	32.2	21.0	32.4
4c	$C_2B_3H_5 + NH_3$	−0.5	−18.6	−24.1
5a	$C_2B_3H_7{\cdot}NH_3$	0.0	0.0	0.0
5b	$C_2B_3H_7 + NH_3$	5.9	−6.3	5.7
5c	$C_2B_3H_7{\cdot}NH_3$	38.8	36.0	26.1
5d	$C_2B_3H_7 + NH_3$	4.8	−11.9	−9.6

Table III. Calculated B–N Bond Lengths (Å) and Bond Strengths (kcal/mol)

		B–N[a]	3-21G	6-31G*	MP2/6-31G*	valency[b]
	$BH_3{\cdot}NH_3$	1.714	35.6	24.3	35.2	2.81
1a	$B_3H_7{\cdot}NH_3$	1.676	40.9	29.0	42.9	2.99
1c	$B_3H_7{\cdot}NH_3$	1.720	32.5	21.3	33.5	2.83
2a	$B_4H_8{\cdot}NH_3$	1.677	40.9	28.9	43.2	2.99
2c	$B_4H_8{\cdot}NH_3$	1.713	33.7	22.8	36.4	2.86
3a	$B_5H_9{\cdot}NH_3$	1.68[c]		21.5	35.8	3.11
4a	$C_2B_3H_5{\cdot}NH_3$	1.697	32.2	21.0	32.4	2.98
5a	$C_2B_3H_7{\cdot}NH_3$	1.632	5.9	−6.3	5.7	3.71
5c	$C_2B_3H_7{\cdot}NH_3$	1.673	−34.0	−47.9	−35.7	3.56

[a] Calculated B–N bond length at the HF/3-21G level. [b] Valency calculated for the unadducted boron hydride or carborane by the MNDO method: Armstrong, D. R.; Perkins, P. G.; Stewart, J. J. P. *J. Chem. Soc., Dalton Trans.* **1973**, 838–840. [c] Assumed.

The purpose of the present contribution is to explore the nature of complexes formed between a boron hydride or carborane and NH_3, which is an example of a good nucleophile. All calculations were carried out by using the GAUSSIAN 82 or GAUSSIAN 86 program systems.[8,9] Geometries were optimized at the HF/3-21G level and single-point calculations made at the MP2/6-31G* level.[10] Total energies are given in Table I, relative energies in Table II, and calculated geometric parameters in Figure 1. Zero-point-energy corrections, which have not been included, would be expected to reduce the difference between reactants and complex. In order to determine the preferred orientation of the NH_3 group, MNDO[11] calculations were carried out. The lowest energy conformation was then used as a starting point for the complete ab initio optimization at the HF/3-21G level.

---

(6) Camp, R. N.; Marynick, D. S.; Graham, G. D.; Lipscomb, W. N. *J. Am. Chem. Soc.* **1978**, *100*, 6781.

(7) McKee, M. L.; Lipscomb, W. N. *Inorg. Chem.* **1985**, *24*, 765–767. Gaines, D. F.; Coons, D. E. *J. Am. Chem. Soc.* **1985**, *107*, 3266–3271 and references cited therein.

(8) Binkley, J. A.; Frisch, M.; Raghavachari, K.; Fluder, E.; Seeger, R.; Pople; J. A. *GAUSSIAN 82*; Carnegie-Mellon University: Pittsburgh, PA, 1982.

(9) Frisch, M.; et al. *GAUSSIAN 86*; Carnegie-Mellon Quantum Chemistry Publishing Unit, Carnegie-Mellon University: Pittsburgh, PA, 1984.

(10) For a description of basis sets, see: Hehre, W. J.; Radom, L.; Schleyer, P. v. R.; Pople, J. A. *Ab Initio Molecular Orbital Theory*; Wiley: New York, 1986.

(11) Dewar, M. J. S.; Thiel, W. *J. Am. Chem. Soc.* **1977**, *99*, 4899.

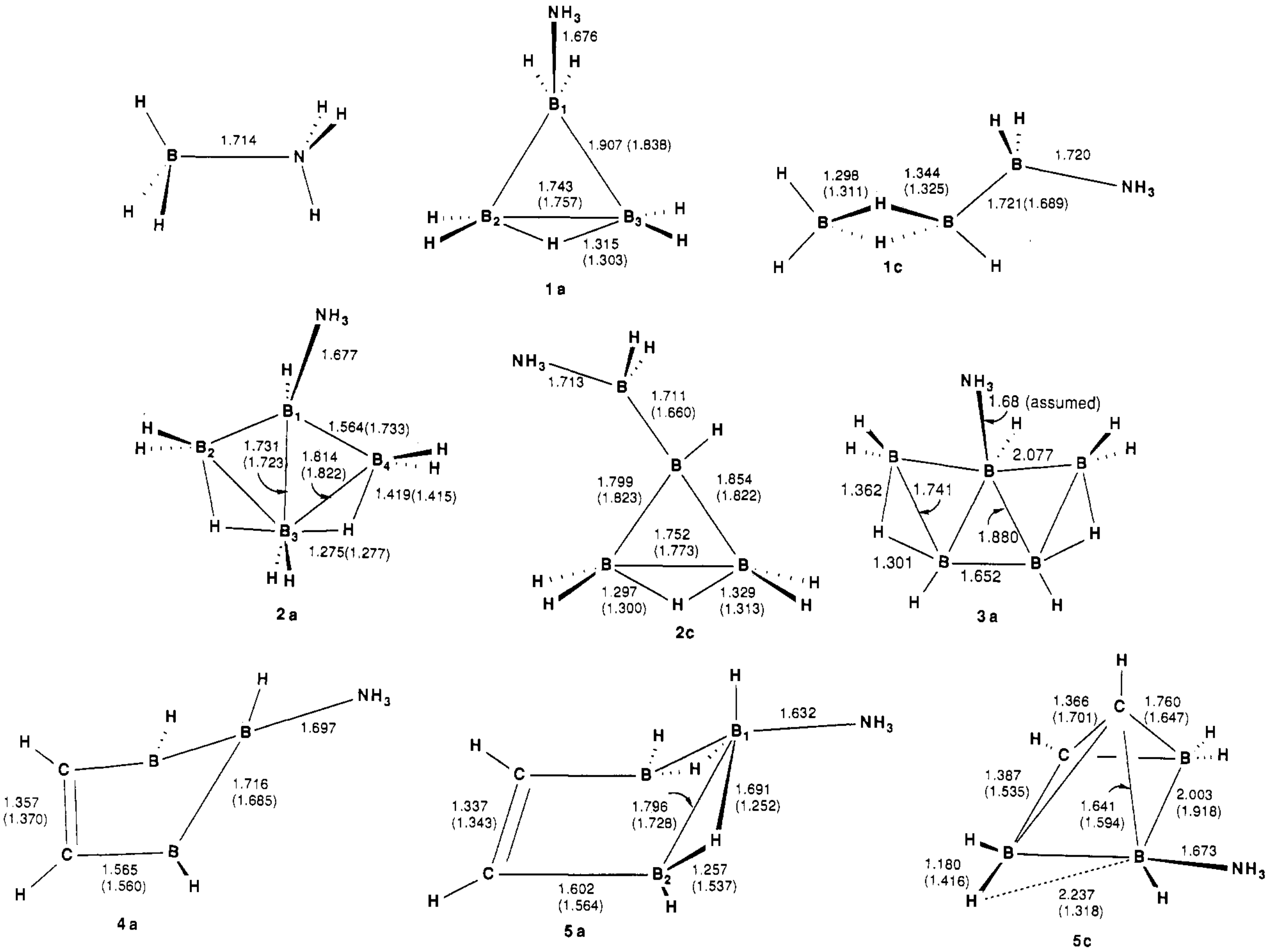

Figure 1. Selected geometric parameters for various stationary structures at the HF/3-21G level. Values in parentheses refer to the optimized parameters in the corresponding noncomplexed structure.

$BH_3·NH_3$. The simplest B–N adduct is $BH_3·NH_3$, which has been well studied theoretically.[12-14] The complexation energy is calculated to be 35.2 kcal/mol, which is in excellent agreement with higher level calculations (34.7,[12] 30.2,[13] and 27.6[14] kcal/mol) and an experimental value of 30.9 kcal/mol.[15] This value is 5.0 kcal/mol smaller than the calculated dimerization energy of B_2H_6[16] at the same level of theory, which compares well with a 4.9 kcal/mol difference calculated by Bartlett and co-workers.[13] The B–N bond is calculated (HF/3-21G) to be slightly longer than the B–N bond determined by microwave spectroscopy[17] (1.714 Å, theory; 1.658 Å, microwave spectroscopy).

$B_3H_7·NH_3$ and $B_4H_8·NH_3$. The boron hydrides B_3H_7 and B_4H_8 have been postulated as intermediates in the pyrolysis of B_2H_6.[18,19] Neither has been experimentally observed. However, both are known as adducts with various nucleophiles ($B_3H_7·L$, L = NH_3[20] and CO;[21] $B_4H_8·L$, L = PF_2NMe_2[22]). In previous studies[23-26] where the geometries of the free boron hydrides B_3H_7 and B_4H_8 were compared, a doubly bridged species was found to be most stable for B_3H_7 and a triply bridged species was found to be most stable for B_4H_8.

Table IV. Comparison of the Calculated Geometry (Å) of $B_3H_7·NH_3$ (**1a**) and $B_4H_8·NH_3$ (**2a**) with the X-ray Structure of $B_3H_7·NH_3$ and $B_4H_8PF_2·NMe_2$

$B_3H_7·L$			$B_4H_8·L$		
param	theory	X-ray[a]	param	theory	X-ray[c]
B_1–B_3	1.907	1.81	B_1–B_3	1.731	1.67
B_2–B_3	1.743	1.74	B_3–B_4	1.814	1.75[b]
B_2–H_b	1.315	1.31[b]	B_1–B_4	1.564	1.82[b]
B_1–N	1.676	1.58	B_4–H_b	1.419	1.27[b]
			B_3–H_b	1.275	1.12[b]

[a] Reference 20. [b] Average of two bond lengths in adduct. [c] Reference 22.

Two previous calculations of a B_3H_7 adduct have been reported: one considered the nucleophile CO[27] and the other considered NH_3.[28] In the present work two alternative modes of NH_3 attachment have been considered (**1a,c**). In one, NH_3 is complexed to the empty orbital of a BH_2 group in a BH_2-substituted diborane (**1c**). At the MP2/6-31G* level this adduct is 14.5 kcal/mol less stable than the structure that is similar to the experimentally observed adduct (**1a**). The strength of the more stable B–N bond

---

(12) Binkley, J. S.; Thorne, L. R. *J. Chem. Phys.* **1983**, *79*, 2932–2940.
(13) Redmon, L. T.; Purvis, L. D., III; Bartlett, R. J. *J. Am. Chem. Soc.* **1979**, *101*, 2856–2862.
(14) Zirz, C.; Ahlrichs, R. *J. Chem. Phys.* **1981**, *75*, 4980–4982.
(15) Umeyama, H.; Morokuma, K. *J. Am. Chem. Soc.* **1976**, *98*, 7208.
(16) For recent high-level calculations of the dimerization energy, see: (a) DeFrees, D. J.; Raghavachari, K.; Schlegel, H. B.; Pople, J. A.; Schleyer, P. v. R. *J. Phys. Chem.* **1987**, *91*, 1857–1864. (b) Page, M.; Adams, G. F.; Binkley, J. S.; Melius, C. F. *J. Phys. Chem.* **1987**, *91*, 2675–2678. (c) Stanton, J. F.; Bartlett, R. J.; Lipscomb, W. N. *Chem. Phys. Lett.* **1987**, *138*, 525–530.
(17) Thorne, L. R.; Suenram, R. D.; Lovas, F. J. *J. Chem. Phys.* **1983**, *78*, 167–171.
(18) Fehlner, T. P. In *Boron Hydride Chemistry*; Muetterties, E. L., Ed.; Academic: New York, 1975; p 175.
(19) Greenwood, N. N.; Greatrex, R. *Pure Appl. Chem.* **1987**, *59*, 857–868.
(20) (a) Nordman, C. E. *Acta Crystallogr.* **1957**, *10*, 777. (b) Nordman, C. E.; Reimann, C. *J. Am. Chem. Soc.* **1959**, *81*, 3538.
(21) Glore, J. D.; Rathke, J. W.; Schaeffer, R. *Inorg. Chem.* **1973**, *12*, 2175.
(22) LaPrade, M. D.; Nordman, C. E. *Inorg. Chem.* **1969**, *8*, 1669.
(23) McKee, M. L.; Lipscomb, W. N. *Inorg. Chem.* **1982**, *21*, 2846–2850.
(24) (a) Ortiz, J. V.; Lipscomb, W. N. In *AIP Conference Proceedings 140* (*Boron-Rich Solids*); American Institute of Physics: New York, **1986**; pp 274–287. (b) Ortiz, J. V.; Lipscomb, W. N. *Chem. Phys. Lett.* **1983**, *103*, 59–62.
(25) Pepperberg, I. M.; Halgren, T. A.; Lipscomb, W. N. *Inorg. Chem.* **1977**, *16*, 363–379.
(26) Lipscomb, W. N. *Pure Appl. Chem.* **1977**, *49*, 701–716.
(27) Brown, L. D.; Lipscomb, W. N. *Inorg. Chem.* **1977**, *16*, 1–7.
(28) Armstrong, D. R. *Inorg. Chim. Acta* **1976**, *18*, 13–18.

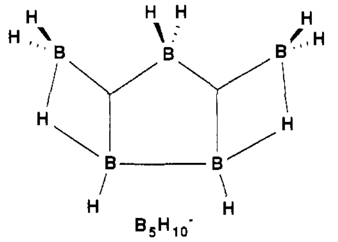

$B_5H_{10}^-$

Figure 2. Optimized structure of $B_5H_{10}^-$ that is based on a C_2 symmetry model for skeletal rearrangement in B_5H_9 to which a hydride has been added at the central boron.

is calculated to be 42.9 kcal/mol, which is 7.7 kcal/mol stronger than the B–N bond in $BH_3{\cdot}NH_3$. The symmetrized X-ray structure[20] is compared to the calculated geometry in Table IV. The boron to which NH_3 is attached is predicted to be substantially farther from the basal borons than found in the crystal structure (1.907 Å, theory; 1.81 Å, X-ray). The apical $BH_2{\cdot}NH_3$ unit is bonded to the basal H_2BHBH_2 fragment by a three-center two-electron bond which may not be adequately described at the HF/3-21G level. However, it is known that large geometric displacements in electron-deficient bonds may result in modest changes in energy,[29] which is in contrast to most organic compounds where two-center two-electron bonding prevails. In these compounds a lengthening of one bond reduces the three-center two-electron description of the interaction and at the same time increases the two-center two-electron description. The average of the hydrogen-bridge distances, which are asymmetric in the X-ray structure (1.39, 1.23 Å), is a good agreement with theory (1.315 Å, theory; 1.31 Å, X-ray). The B–N distance is again overestimated (1.676 Å, theory; 1.58 Å, X-ray).

The predicted geometry for the lowest energy adduct of B_4H_8 (**2a**) is in agreement with an X-ray structure for $B_4H_8PF_2{\cdot}NMe_2$.[22] This adduct is 19.2 kcal/mol more stable than a BH_2-substituted triborane in which the NH_3 is coordinated to the unsaturated BH_2 unit (**2c**). A comparison of the $B_4H_8{\cdot}NH_3$ complex and the X-ray structure is made in Table IV. The unbridged boron–boron distances are predicted to be significantly shorter in the NH_3 adduct than in the X-ray-structure of $B_4H_8PF_2{\cdot}NMe_2$ (1.56 Å, theory; 1.82 Å, X-ray). A B–N bond strength of 43.2 kcal/mol is predicted for $B_4H_8{\cdot}NH_3$, which is similar to the 42.9 kcal/mol bond in $B_3H_7{\cdot}NH_3$.

$B_5H_9{\cdot}NH_3$. While a Lewis base adduct of B_5H_9 is known[2] where L = $N(CH_3)$, the complex calculated here for $B_5H_9{\cdot}NH_3$ is based on a suggested transition state for skeletal rearrangement in B_5H_9.[7] The geometry for the complex was obtained by first optimizing $B_5H_{10}^-$ in C_2 symmetry (Figure 2), where the Lewis base H^- allows symmetry to be imposed. The NH_3 complex was then calculated with this geometry by replacing H^- with NH_3 and assuming a B–N distance of 1.68 Å. The full optimization of $B_5H_9{\cdot}NH_3$ in C_1 symmetry would be too time consuming, and the errors introduced by determining the adduct geometry with hydride as the Lewis base rather than NH_3 should be small.

The complex (**3a**) is predicted to be 35.8 kcal/mol more stable than the C_2 model plus NH_3 (**3b**) at the MP2/6-31G* level, but it is still 11.5 kcal/mol less stable than the known C_{4v} structure plus NH_3 (**3c**). This would nicely rationalize the significantly lower skeletal rearrangement barrier in coordinating solvents. The C_{4v} structure would not likely be stabilized while the transition state is greatly stabilized. At the MP2/6-31G* level the barrier would be reduced from 47.3 kcal/mol (in the gas phase) to 11.5 kcal/mol (in a good coordinating solvent) if the C_2 model can be taken as the transition state both in the gas phase and in solution.

$C_2B_3H_5{\cdot}NH_3$ and $C_2B_3H_7{\cdot}NH_3$. Carboranes are known to interact with Lewis bases.[4,5] As an example of a coordinated carborane, an envelope-like structure of $C_2B_3H_5$ was optimized with NH_3 complexed to the unsaturated boron (**4a**). Although the B–N bond strength in the complex is 32.4 kcal/mol, the closo carborane, 1,5-$C_2B_3H_5$, plus NH_3 is still 24.1 kcal/mol more stable than the complex at the MP2/6-31G* level (Table II). Therefore, it is not likely that the carborane will form an adduct in a coordinating solvent. An NH_3–closo carborane complex was sought, but the starting geometry optimized to separate moieties at the HF/3-21G level.

The known geometry of $C_2B_3H_7$ is a carbon-capped square with a pair of hydrogen bridges on the perimeter.[4] An envelope-like structure (**5a**) was found that was only slightly less stable at the HF/3-21G level (Table II). The NH_3 adduct of this structure is more stable than the known $C_2B_3H_7$ structure plus NH_3 at the HF/3-21G level. However, the stabilities switch at higher level, and at the MP2/6-31G* level the known structure plus NH_3 is 9.6 kcal/mol more stable than the adduct.

It should be noted that a metal can also stabilize the classical form of a boron hydride or carborane. As an example, it is known[30] that the reaction of $C_2B_6H_8$ and $Fe(CO)_5$ produces a complex consisting of the five-membered-ring $C_2B_3H_7$ ligand coordinated to $Fe(CO)_3$. A comparison of the calculated free and adducted geometry of **5c** is made with the X-ray structure[31] in Table V. Also, a description of the electronic structure of the complex has appeared.[32]

Table V. Comparison of the Calculated Geometry (Å) of $C_2B_3H_7$ (**5c**) with the X-ray Structure of $C_2B_3H_7{\cdot}Fe(CO)_3$

	theory		X-ray[a]
param	$C_2B_3H_7$	$C_2B_3H_7{\cdot}NH_3$	$C_2B_3H_7{\cdot}Fe(CO)_3$
B_1–B_2	1.728	1.796	1.852
B_2–C	1.564	1.602	1.520
C–C	1.343	1.337	1.410
B_1–H_b	1.252	1.691	1.25
B_2–H_b	1.537	1.257	1.26

[a] Reference 31.

A bond strength of 5.7 kcal/mol was calculated for the B–N bond in the complex, which is much weaker than other calculated B–N bond strengths. Undoubtedly, the reason for the small bond strength is that the boron is already nearly coordinatively saturated in the free form. While the bond strength is small, the complex may have kinetic stability because the complex has the shortest B–N bond length of all adducts calculated (1.632 Å). An NH_3 complex with the carbon-capped square structure (**5c**) was also found with a B–N bond length of 1.673 Å. The major geometry change in the carborane upon complexation with NH_3 is that both bridging hydrogens become terminal. The B–N bond energy is negative at all levels, which indicates that the adduct is less stable than the carborane plus NH_3.

General Observations. Complexation by ammonia is most stabilizing for structures that have a vacancy on boron. On the basis of a small sample, stabilizations fall into three groups. A stabilization of 32.4–36.4 kcal/mol results from the complexation of NH_3 to RBH_2 where all bonds to boron are two-center two-electron. The 35.8 kcal/mol B–N bond strength in $B_5H_9{\cdot}NH_3$ (**3a**) involves a BH unit attached by two three-center two-electron bonds. A larger stabilization of 42.9–43.2 kcal/mol results when NH_3 complexes to a BH_2 unit that is bonded by a single three-center two-electron bond to the rest of the molecule. Bonds with little or no thermodynamic stability result when NH_3 is complexed to a coordinatively saturated boron. The latter point is made by comparing the valency calculated by MNDO for the free boron hydride or carborane (Table III). In each case the thermodynamically weak B–N bond is attached to a boron center that is already coordinatively rich.

The B–N bond lengths are predicted to be longer than those found by X-ray diffraction. The range of B–N bond lengths to RBH_2 (all bonds two-center two-electron) is from 1.713 to 1.720 Å, an overestimation of about 0.05 Å. When the BH_2 unit is connected by a three-center two-electron bond to the rest of the molecule, the bond shortens to 1.676–1.677 Å. Bonds to saturated

---

(29) McKee, M. L.; Lipscomb, W. N. *Inorg. Chem.* **1981**, *20*, 4442–4444.

(30) Grimes, R. N. *J. Am. Chem. Soc.* **1971**, *93*, 261–262.

(31) Brennan, J. P.; Grimes, R. N.; Schaffer, R.; Sneddon, L. G. *Inorg. Chem.* **1973**, *12*, 2266–2268.

(32) Armstrong, D. R.; Findlay, R. H. *Inorg. Chim. Acta* **1977**, *21*, 55–59.

boron centers are thermodynamically weak but may be short (1.632–1.697 Å), indicating possible kinetic stability.

In the case of reactive boron hydrides (BH_3, B_3H_7, and B_4H_8) the complex is more stable than the boron hydride plus NH_3, while in the case of the observed carboranes ($C_2B_3H_5$, $C_2B_3H_7$) and B_5H_9 the complex is less stable than the observed free species plus NH_3.

Acknowledgment. We thank the donors of the Petroleum Research Fund, administered by the American Chemical Society, for financial support. Computer time for this study was also donated by the Auburn University Computer Center. Drs. U. Peter and T. Webb are thanked for a careful reading of the manuscript.

Contribution from the Department of Chemistry,
Purdue University, West Lafayette, Indiana 47907

Localized States in Reduced and Excited-State Ruthenium(II) Terpyridyls

Robert M. Berger and David R. McMillin*

Received February 24, 1988

Spectroelectrochemical studies of Ru(trpy)(bpy)(py)$^{2+}$ and Ru(trpy)(4,4′-dph-bpy)(py)$^{2+}$ (trpy = 2,2′:6′,2″-terpyridine, bpy = 2,2′-bipyridine, 4,4′-dph-bpy = 4,4′-diphenyl-2,2′-bipyridine, py = pyridine) as well as the corresponding homoleptic polypyridyl complexes have been carried out. The results show that one-electron reduction of the mixed-ligand complexes involves introducing an electron into a π^* orbital that is essentially localized on the trpy ligand system. Low-temperature EPR spectra support this interpretation and together with the other data suggest that the electron is localized on a single trpy ligand in Ru(trpy)$_2^+$ as well. Finally, the linear correlation between the energy of the MLCT emission maximum and the difference in potential between the first oxidation and reduction waves of these complexes indicates that the same ligand orbital is populated in the lowest energy metal-to-ligand charge-transfer excited state.

Introduction

Since the first report[1] of luminescence from Ru(bpy)$_3^{2+}$ (bpy = 2,2′-bipyridine), the photophysical and photochemical properties of this and related d^6 polypyridyl complexes have been the subject of intense interest.[2–18] Two models of the emitting metal-to-ligand charge-transfer (MLCT) excited states of Ru(bpy)$_3^{2+}$ have been proposed. One of these involves the symmetric delocalization of the transferred electron density over all three bipyridine ligands (delocalized model).[2] In the other, so-called localized model, the transferred electron density tends to be found on only one of the bipyridines, but it can "hop" from ligand to ligand. Excited-state absorption[5] and transient circular dichroism measurements[6] as well as steady-state[11] and time-resolved[12] photoselection measurements are consistent with localization. Perhaps the strongest evidence for a localized excited state, however, comes from the time-resolved resonance Raman (TR^3) spectrum of the excited state at room temperature[13] or in a rigid ethanol/methanol glass.[14] These experiments clearly establish that localization occurs on at least a nanosecond and even a picosecond[14a] time scale. The photophysics and photochemistry of the related 2,2′:6′,2″-terpyridine (trpy) complexes have received far less attention, although these species are interesting in their own right.[19–22] It has, however, been argued that charge localization can occur in these systems, too.[23] In the excited states of mixed-ligand complexes containing both tridentate and bidentate polypyridine ligands, charge localization is certainly expected; however, the questions remain as to which ligand is favored and to what extent substituents influence the localization. A priori, trpy, with a more extended π-system than bpy, would be expected to present a more energetically accessible π^* orbital and hence a lower energy excited state. In an attempt to answer this question for Ru(trpy)(bpy)(py)$^{2+}$ (py = pyridine) and related systems, we have at-

---

(1) Paris, J. P.; Brandt, W. W. *J. Am. Chem. Soc.* **1959**, *81*, 5001.

(2) (a) Harrigan, R. W.; Crosby, G. A. *J. Chem. Phys.* **1973**, *59*, 3468. (b) Hipps, K. W.; Crosby, G. A. *J. Am. Chem. Soc.* **1975**, *97*, 7042. (c) Ferguson, J.; Krausz, E. *Inorg. Chem.* **1987**, *26*, 1383. (d) Ferguson, J.; Krausz, E. *Inorg. Chem.* **1986**, *25*, 3333. (e) Yersin, H.; Gallhuber, E. *J. Am. Chem. Soc.* **1984**, *106*, 6582.

(3) Braterman, P. S.; Heath, G. A.; Yellowlees, L. J. *J. Chem. Soc., Dalton Trans.* **1985**, 1081.

(4) Kober, E. M.; Meyer, T. J. *Inorg. Chem.* **1982**, *21*, 3967.

(5) DeArmond, M. K. *Acc. Chem. Res.* **1974**, *7*, 309.

(6) Gold, J. S.; Milder, S. J.; Lewis, J. W.; Kliger, D. S. *J. Am. Chem. Soc.* **1985**, *107*, 8285.

(7) (a) Van Houten, J.; Watts, R. J. *Inorg. Chem.* **1978**, *17*, 3381. (b) Van Houten, J.; Watts, R. J. *J. Am. Chem. Soc.* **1976**, *98*, 4853.

(8) (a) Balzani, V.; Bolletta, F.; Gandolfi, M. T.; Maestri, M. *Top. Curr. Chem.* **1978**, *75*, 1. (b) Juris, A.; Balzani, V.; Barigelletti, F.; Campagna, S.; Belser, P.; von Zelewsky, A. *Coord. Chem. Rev.* **1988**, *84*, 85.

(9) Sutin, N.; Creutz, C. *Adv. Chem. Ser.* **1978**, *No. 168*, 1.

(10) (a) Meyer, T. J. *Acc. Chem. Res.* **1978**, *11*, 94. (b) Meyer, T. J. *Pure Appl. Chem.* **1986**, *58*, 1193.

(11) Carlin, C. M.; DeArmond, M. K. *J. Am. Chem. Soc.* **1985**, *107*, 53.

(12) Myrick, M. L.; Blakley, R. L.; DeArmond, M. K. *J. Am. Chem. Soc.* **1987**, *109*, 2841.

(13) (a) Dallinger, R. F.; Woodruff, W. H. *J. Am. Chem. Soc.* **1979**, *101*, 4391. (b) Bradley, P. G.; Kress, N.; Hornberger, B. A.; Dallinger, R. F.; Woodruff, W. H. *J. Am. Chem. Soc.* **1981**, *103*, 7441.

(14) (a) Carroll, P. J.; Brus, L. E. *J. Am. Chem. Soc.* **1987**, *109*, 7613. (b) Stacy, N. E.; Berger, R. M.; Dallinger, R. F., unpublished results.

(15) Kalyanasundaram, K. *Coord. Chem. Rev.* **1982**, *46*, 159.

(16) Motten, A. G.; Hanck, K. W.; DeArmond, M. K.; *Chem. Phys. Lett.* **1981**, *79*, 541.

(17) (a) DeArmond, M. K.; Hanck, K. W.; Wertz, D. W. *Coord. Chem. Rev.* **1985**, *64*, 65. (b) Angel, S. M.; DeArmond, M. K.; Donohoe, R. J.; Hanck, K. W.; Wertz, D. W. *J. Am. Chem. Soc.* **1984**, *106*, 3688.

(18) Heath, G. A.; Yellowlees, L. J.; Braterman, P. S. *J. Chem. Soc., Chem. Commun.* **1981**, 287.

(19) Demas, J. N.; Crosby, G. A. *J. Am. Chem. Soc.* **1971**, *93*, 2841.

(20) Stone, M. L.; Crosby, G. A. *Chem. Phys. Lett.* **1981**, *79*, 169.

(21) Kirchhoff, J. R.; McMillin, D. R.; Marnot, P. A.; Sauvage, J. P. *J. Am. Chem. Soc.* **1985**, *107*, 1138.

(22) (a) Young, R. C.; Nagle, J. K.; Meyer, T. J.; Whitten, D. G. *J. Am. Chem. Soc.* **1978**, *100*, 4773. (b) Allen, G. H.; Sullivan, B. P.; Meyer, T. J. *J. Chem. Soc., Chem. Commun.* **1981**, 793.

(23) (a) Braterman, P. S. *Chem. Phys. Lett.* **1984**, *104*, 405. (b) Morris, D. E.; Hanck, K. W.; DeArmond, M. K. *J. Electroanal. Chem. Interfacial Electrochem.* **1983**, *149*, 114.

0020-1669/88/1327-4245$01.50/0